Atmospheric models, GPS and InSAR measurements of the tropospheric water vapour field over Mount Etna

G. Wadge[1], P.W. Webley[1], I.N. James[2], R. Bingley[3], A. Dodson[3], S. Waugh[3], T. Veneboer[3], G. Puglisi[4], M. Mattia[4], D. Baker[3], S.C. Edwards[5], S.J. Edwards[5], P.J. Clarke[5]

1. Environmental Systems Science Centre, University of Reading
   Harry Pitt Building, 3 Earley Gate, Reading RG6 6AL, U.K.
   tel: +44 1189 318741, fax: +44 1189 316413, email: gw@mail.nerc-essc.ac.uk
2. Department of Meteorology, University of Reading, U.K.
3. Institute of Engineering Surveying and Space Geodesy, University of Nottingham, U.K.
4. Istituto Nazionale di Geofisica e Vulcanologia, Catania, Italy
5. Department of Geomatics, University of Newcastle upon Tyne, U.K.

Abstract

Dynamic models of atmospheric movement over the Mount Etna volcano are used to calculate the path delays affecting radar caused by variable water vapour in the troposphere. We compare these model results with the equivalent differential radar interferogram generated by two ERS-2 SAR images taken 35 days apart and the water vapour delay retrievals from a network of fourteen GPS stations distributed over the volcano. The atmospheric model delay field agrees well with the long-wavelength spatial differences measured by InSAR and those measured by GPS.

Index Terms

1243-Space geodetic surveys, 3367-Atmospheric theoretical modeling, 6924- Interferometry, 6964-Radio wave propagation.

Introduction

The spatial and temporal variability of tropospheric water vapour modifies the refractivity of radio waves passing between satellites and the ground. The temporal variability can be measured by GPS, but the spatial variability is a major source of noise for radar interferometry (InSAR) used in repeat-pass mode to detect ground surface motions [*Hanssen*, 2001]. The effect should be particularly strong over mountains because of the variable tropospheric path length and the local flow of air induced by the topography. Two types of technique are used to reduce this noise in InSAR: statistical, in which multiple data are used to reduce the unwanted component; and calibratory, in which independent measurements are made and used to subtract the atmospheric noise from the ground signal [*Williams et al.*, 1998]. Here we report on a new calibratory approach to this problem in which we use forward models of the atmospheric flow over a mountain from which we extract the integrated water vapour (IWV) contents along the radar paths. We compare the delays on these paths with an ERS-2 SAR-derived interferogram of 35 days separation and the results of an experiment to measure water vapour delays at a dense array of GPS stations [*Webley et al.,*2002]. The spatial variation of path delay (in mm) between two points on the ground, a and b, is given by $\delta_{a,b}$ and the equivalence of measurements using the three techniques is :

$$\delta_{a,b} = IWV_{a,b} \times Q = \lambda \times \phi_{a,b} / 4\pi = SWD_{a,b}$$

where IWV is the difference in integrated water vapour content in kg m^{-2} along the radar paths through the atmospheric models, Q is an empirically-derived constant (e.g. *Emardson and Derk*s, 2000), ϕ is the interferogram phase difference in radians, λ is the radar wavelength (56mm), and SWD is the slant water delay difference in mm calculated at a GPS station and mapped onto the radar paths. The study site is the 3.3 km high volcano Mount

Etna in Sicily (Fig. 1) which is known to have InSAR-measurable ground movement signals [*Massonnet et al*., 1995] that are susceptible to atmospheric noise of several tens of mm of delay [*Delacourt et al*., 1998, *Beauducel et al*., 2000, *Bonforte et al.,* 2001].

InSAR Measurements by ERS-2

Two ERS-2 SAR images of Etna were acquired during descending passes of the satellite with 35 days separation on 6 September and 11 October 2000 at 09:41 UTC (Track 222/Frame 2853/Orbits 28132 and 28633). The SAR images were processed interferometrically with PULSAR software using precise information from the ESA PRC products for orbital positioning and velocity. The effect of topography was removed using a high resolution DEM with an rms height uncertainty of about 5m. The resulting differential interferogram with a resolution of 60m was filtered adaptively [*Goldstein and Werner*, 1998] and unwrapped with a branch-cut algorithm. Areas of low phase correlation and consequent difficulty in phase unwrapping were masked, reducing the information retrieved from the eastern side of the volcano. The phase standard deviation of the selected area is about 1.5 radians (equivalent to a path difference of about 7 mm) based on the coherence of the scene and the assumption of a perfect distributed scattering surface [*Just and Bamler*, 1994]. The line of sight of the radar during the descending pass is about 23^o from the vertical directed just north of west and is given by the unitary vector (east = -0.373, north = -0.077, up = 0.925). Volcanic activity on Etna during this 35 day period consisted of ash emission in mid-September, similar to activity before and afterwards, and we have no reason to think that any relative surface deformation during this period was above the level of a few millimetres. We, therefore, assume that the phase changes measured by InSAR are due to water vapour effects in the troposphere.

Atmospheric Modelling

Numerical models of the atmosphere used for weather prediction are too coarse to represent the km-scale features that might affect the water vapour field over a mountain. Instead we have used a higher resolution, limited area model designed to incorporate representative orography of the mountain at the base of the model space. This NH3D model [*Miranda and James*, 1992] uses the non-hydrostatic equation set of Miller and White [1984] with terrain-following coordinates. Water vapour is treated as a passive tracer and so no explicit account is taken of cloud formation or precipitation. The model space is centred on Etna, has horizontal dimensions of 110 x110 at 1.7 km per cell and 30 vertical levels with absorption layers in those uppermost and a free-slip lower boundary condition. Initialisation of the models uses temperature, wind vectors and specific humidity data from the nearest radiosonde station at Trapani which is about 150 km west of the western face of the model space (Fig. 1) and is the commonest upwind direction for Etna. Radiosonde records are available every six hours at Trapani. Ideally, a record corresponding to the air mass that will be advected over Etna at the time of the overpass is required. The radiosonde records from either eleven or five hours before overpass are suitable. The topography around Etna was extracted from the GTOPO30 DEM with a pixel size of about 860m. At the outer base of the model space the topography was smoothed to help stabilise the initial stages of the flow and the full topography was grown incrementally during each simulation for the same reason.

On 6 September 2000 the wind was from the northwest. On 10 October 2000 the wind was from the southwest and the general humidity levels were greater. Using radiosonde data from five hours before the radar acquisitions NH3D was run for about ten hours per simulation at 4 s time steps. The models become more stable after a few hours of run time and variance levels over Etna are typically very much less than 10% of the simulated humidity field. Figure 2 shows a down-wind vertical profile of the specific humidity field of the model run for 10 October 2000. Moist air is advected up the western slopes and an intrusion of dry air descends the eastern side of the volcano. The lee sides of the volcano generally show more complex flow patterns and variable water vapour fields. For comparison with the InSAR results we calculated the NH3D IWV contents along the radar paths through the model troposphere projected onto the surface of Etna and converted these to equivalent path delays using a Q factor of 6.3 [*Webley et al*., 2002]. Differencing of the delay maps for the two dates gives a spatial result that can be compared to that from differential InSAR (Fig. 3).

GPS Experiment

Fourteen geodetic GPS receivers with choke-ring antennas were deployed in continuous mode on Etna during two ten-day periods between August and October 2000 [*Webley et al*., 2002]. The receivers occupied sites ranging from approximately 50-3000 m above sea level (Fig. 1). Measurement epochs of 30 s with cut-off angles of 15^{o} were used and nearly complete recovery of data from the network was achieved. Surface meteorological measurements were made simultaneously at one site (SLN1).

Processing of the GPS data was carried out by both IESSG GPS Analysis Software (GAS) and the NASA/JPL GIPSY-OASIS II software. For the former the solutions were calculated with respect to the IGS station at Matera in southern Italy which was fixed in the ITRF97 reference frame. The ionospherically-free observable was used and corrections for solid earth tides applied. Zenith Total Delay (ZTD) was estimated per station, as a constant parameter over a 15 minute period using a Kalman filter with a constraint of 0.4 $cm/hr^{0.5}$ and the Niell dry mapping function to map the signal delays to the zenith [*Webley et al*., 2002]. The Zenith Hydrostatic Delay was calculated using the pressure history at SLN1, the height of the stations and the empirical formula of *Saastamoinen* [1972]. Zenith Wet Delay (ZWD) was obtained by difference. We also calculated the Slant Wet Delay (SWD) values along the radar paths using the Niell mapping function. Resultant values for the GAS processing (Table 1) were very similar to those from GIPSY-OASIS.

Discussion

The interferogram, the NH3D models and the GPS water vapour calculations are generally consistent with an increase in the tropospheric water vapour content from 6 September to 10 October 2000 at the times of the ERS-2 overpasses of Etna. The spatial pattern and magnitudes of the longer wavelength changes changes shown by the interferogram and the models are similar (Fig. 3 b,c), with a maximum to the south of the volcano and minima to the northeast and southeast of the summit, though the range shown by the model values is about 50% greater than that of the InSAR values. In Table 1 the InSAR delay measurements have been offset to the difference in GPS delays at station BRO9 (which has the lowest GPS value). The relative sense of change of the GPS values is in general agreement with the interferogram where there is overlap. The exception to this is the lowest station IIV1 where the GPS delay value is about 60 mm less than for the other two methods. Subtracting the NH3D values from the InSAR values in Table 1 reduces the rms variance from 46 mm to 18 mm with a mean of -4 mm. The equivalent values for InSAR-GPS give an rms value of 19 mm and a mean of +12 mm.

More exact comparisons between the techniques are difficult. Uncertainty in the knowledge of the satellite orbital positions may leave residual planar trends in the interferogram, though none are obvious here and no empirical adjustment was made. The delay values measured by the GPS network are point representations of the combined paths through the troposphere from the GPS satellites to the receivers. In effect they are the result of an arbitrary sampling of a conical space with its apex at the receiver (see *Hanssen*, [2001], Fig. A.2). As a result of this the SWD difference values will always represent a different and more diffuse sampling of the change in water vapour field than is the case for InSAR values.

The main sources of uncertainty for the NH3D models are the quality and validity of the initialisation parameters. In our first model runs for 10 October 2000 we used the radiosonde record from 11 hours before overpass. However, it is clear from the synoptic weather reports that a weak front passed over Sicily from west to east at about this time and we see evidence of this in an inverted water vapour profile at about 3 km height at Trapani on this radiosonde record and from the GPS water vapour records on the Etna network about 3-6 hours later. This front had passed out of the NH3D model space area by the time of the overpass and thus we used the later Trapani radiosonde record. For both dates the upwind direction was generally westward, justifying using the Trapani radiosonde data. However, for winds from other directions another source of initialisation data would be needed. Numerical weather prediction models may be able to provide this and would give the technique a more general applicability.

We conclude from this study that the path difference effects at Etna can be caused by large horizontal gradients in water vapour that are the result of the advection of air masses up and around the mountain. This is considerably different from the topographic effect on a "static" troposphere [*Delacourt et al*., 1998] and suggests this model approach may be a useful means of correcting InSAR ground motion signals on mountains.

Acknowledgements

This work was supported by NERC grant GR/M86156, NERC studentship GT4/99/222 and also EPSRC grant GR/M86156. The NERC Geophysical Equipment Pool supplied much of our GPS equipment on time and in good order.

References

Beauducel, F., P. Briole and J-L. Froger, Volcano-wide fringes in ERS synthetic aperture radar interferograms of Etna (1992-1998): deformation or tropospheric effect ? *J.Geophys. Res.*, *105*, 16391-16402, 2000.

Bonforte, A., A. Ferretti, C. Prati, G. Puglisi and F. Rocca, Calibration of atmospheric effects on SAR interferograms by GPS and local atmospheric models: first results. *J. Atmos. Solar-Terrestrial Phys., 63,* 1343-1357, 2001.

Delacourt, C., P. Briole and J. Achache, Tropospheric corrections for SAR interferograms with strong topography. Application to Etna. *Geophys. Res. Lett*., *25*, 2849-2854, 1998.

Emardson, T.R. and H.J.P. Derks, On the relation between wet delay and the integrated precipitable water vapour in the European atmosphere. *Meteor. Applications, 7*, 61-68, 2000.

Goldstein, R.M. and C.L. Werner, Radar interferogram filtering for geophysical applications. *Geophys. Res. Lett., 25*, 4035-4038, 1998.

Hanssen, R.F., *Radar Interferometry. Data Interpretation and Error Analysis*, Kluwer, 2001.

Just, D. and R. Bamler, Phase statistics of interferograms with applications to synthetic aperture radar. *Appl. Optics, 33,* 4361-4368, 1994.

Massonnet, D., P. Briole and A. Arnaud, Deflation of Mount Etna monitored by spaceborne radar interferometry. *Nature*, *375*, 567-570, 1995.

Miller, M.J. and A.A. White, On the non-hydrostatic equations in pressure and sigma coordinates. *J.Atmos. Sc*i., *44*, 1775-1800, 1984.

Miranda, P.M.A. and I.N. James, Non-linear three-dimensional effects on gravity-wave drag: splitting flow and breaking waves, *Q.J.R.Meteorol. Soc*., *118*, 1057-1081, 1992.

Saastamoinen, J., Atmospheric correction for the troposphere and stratosphere in radio ranging of satellites. In, *The use of artificial satellites for geodesy*, Geophysical Monograph Series, AGU, Washington D.C., *15*, 247-251, 1972.

Webley, P.W., R.M. Bingley, A.H. Dodson, G. Wadge, S.J. Waugh and I.N. James, Atmospheric water vapour correction to InSAR surface motion measurements on mountains: results from a dense GPS network on Mount Etna. *Phys. Chem. Earth*, (in press), 2002.

Williams, S., Y. Bock and P. Fang, Integrated satellite interferometry: tropospheric noise, GPS estimates and implications for interferometric synthetic aperture radar products. *J.Geophys. Res*., *103*, 27051-27067, 1998.

Table.1 Water vapour delay differences over Etna for 6 September - 10 October, 2000 measured by the three techniques at the GPS sites

Station	Altitude (m asl)	ΔSWD (mm)	InSAR (mm)	ΔNH3D (mm)
IIV1	47	-39	-98	-119
LING	531	-41	-37	-34
ADR8	628	-32	-58	-80
POSE	729	-13	-48	-58
BRO9	734	-46	-46	-54
MAL0	808	-11	-44	-35
MILO	1019	-2	-	-39
EGIT	1569	-30	-37	-62
SPCV	1611	-8	-24	+11
LAMP	1709	-24	-33	-19
SLN1	1731	-10	-31	-20
CIT1	1744	-28	-	-15
OSV1	2824	-19	-10	-33
PLUC	2921	-25	-25	-38

Figure Captions

Fig.1 Distribution of the GPS network on Etna set up in late 2000, shown on a shaded relief model with contours at 250 m intervals. Below is a map of the location of the relief model (thin solid line box), the area of the SAR scene (thick solid line box), the atmospheric model space (dashed line box) and the location of the radiosonde station at Trapani.

Fig.2 Vertical, SW-NE (left-right) section downwind through the NH3D model at the location of the summit of Etna for 10 October 2000 at the time of the ERS-2 overpass. The continuous variable shown is the specific humidity field (units of kg/kg x 10^{-3}) and the yellow arrows are wind vectors. The model topography is shown in white and the top 4km of the model space are not shown.

Fig.3 Comparison of the atmospheric model and the InSAR-measured delays due to water vapour changes between 6 September and 10 October 2000; (a) NH3D model result for the area of Etna with the line representing the section of Fig.2 , (b) NH3D result for same, masked, area as the interferogram, and (c) the unwrapped ERS-2 interferogram.

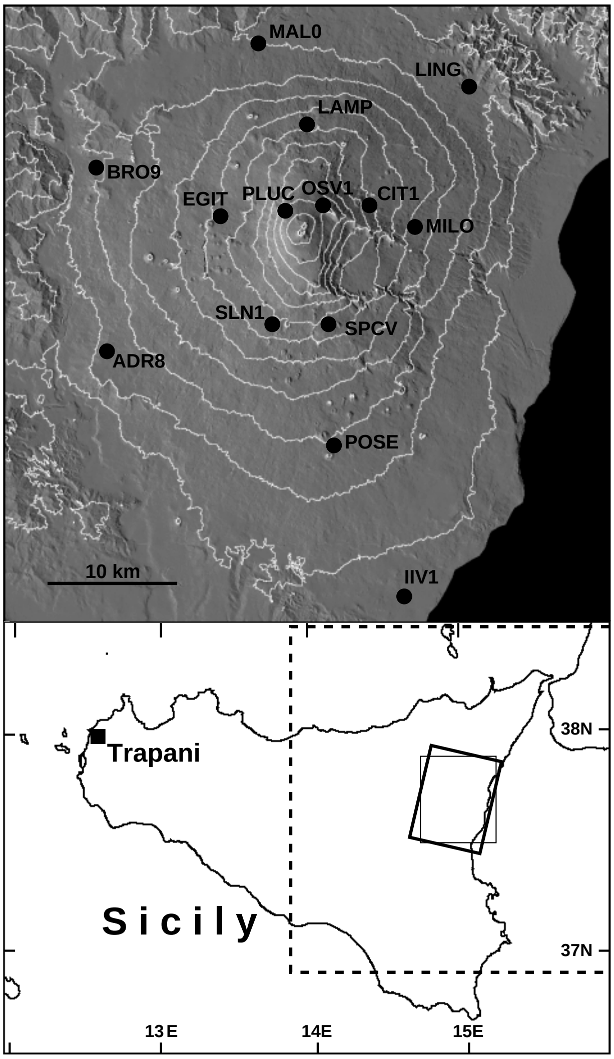
MAL0
LING
LAMP
BRO9
EGIT
PLUC
OSV1
CIT1
MILO
SLN1
SPCV
ADR8
POSE
10 km
IIV1
Trapani
38N
Sicily
37N
13 E
14E
15E

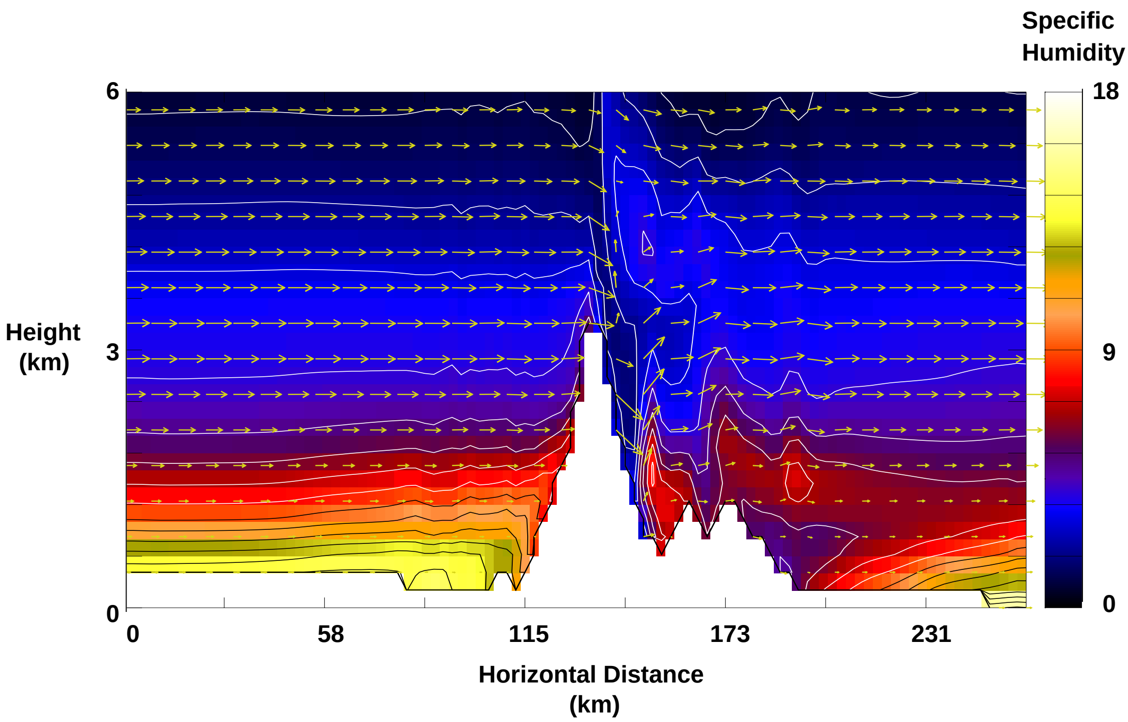
Specific
Humidity
18
9
0
Height
(km)
6
3
0
0
58
115
173
231
Horizontal Distance
(km)

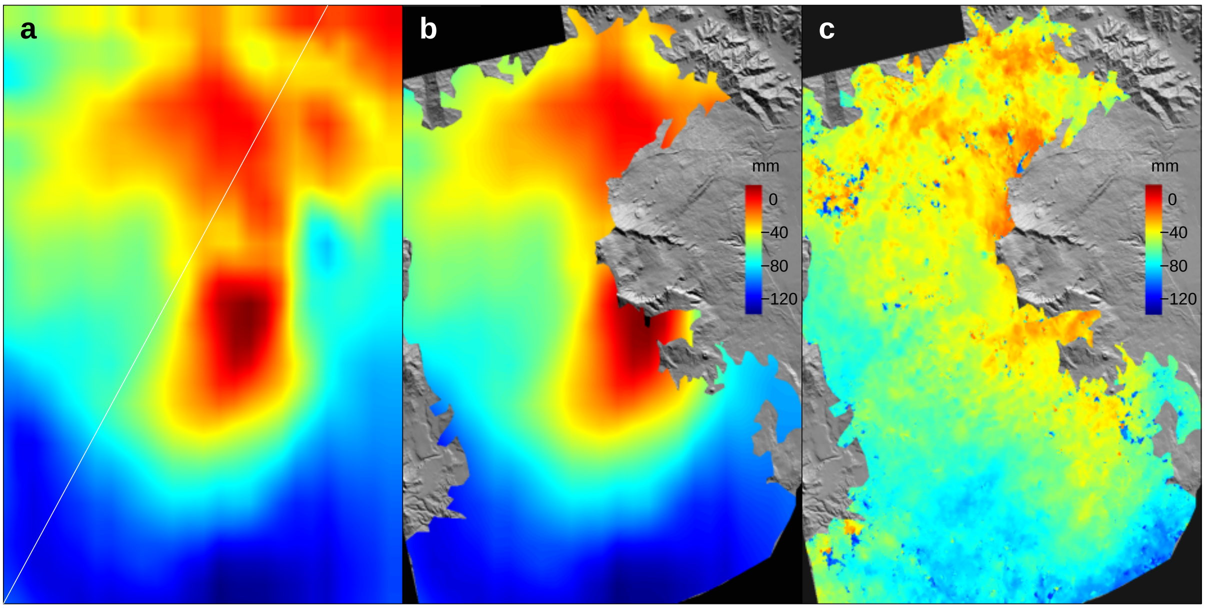
a
b
c
mm
0
-40
-80
-120
mm
0
-40
-80
-120